Journal of Materials Chemistry B

Accepted Manuscript

This is an *Accepted Manuscript*, which has been through the Royal Society of Chemistry peer review process and has been accepted for publication.

Accepted Manuscripts are published online shortly after acceptance, before technical editing, formatting and proof reading. Using this free service, authors can make their results available to the community, in citable form, before we publish the edited article. We will replace this *Accepted Manuscript* with the edited and formatted *Advance Article* as soon as it is available.

You can find more information about *Accepted Manuscripts* in the Information for Authors.

Please note that technical editing may introduce minor changes to the text and/or graphics, which may alter content. The journal's standard Terms & Conditions and the Ethical guidelines still apply. In no event shall the Royal Society of Chemistry be held responsible for any errors or omissions in this *Accepted Manuscript* or any consequences arising from the use of any information it contains.

ROYAL SOCIETY OF CHEMISTRY

www.rsc.org/materialsB

Journal Name

ARTICLE

Electrospun Poly(L-lactide-co-caprolactone)/collagen/chitosan Vascular Graft in a Canine Femoral Artery Model

Received 00th January 20xx,
Accepted 00th January 20xx

DOI: 10.1039/x0xx00000x

www.rsc.org/

Tong Wu[a,1], Bojie Jiang[b,1], Yuanfei Wang[c], Anlin Yin[a], Chen Huang[a], Sheng Wang[b,*], Xiumei Mo[a,*]

Poly(L-lactide-co-caprolactone)/collagen/chitosan (P(LLA-CL)/COL/CS) composite grafts were electrospun in this study. Based on the testing results of mechanical properties, biodegradability and *in vitro* cellular compatibility, the optimal weight ratio of P(LLA-CL) to COL/CS was set as 3:1. *In vivo* study was further performed in a canine femoral artery model. The results showed that the 3:1 grafts possessed excellent structural integrity, higher patency rate, better endothelial cells (ECs) and smooth muscle cells (SMCs) growth, as well as higher gene and protein expression levels of angiogenesis-related cues than those of grafts based on P(LLA-CL). The findings confirmed that the addition of natural materials such as collagen and chitosan could effectively improve endothelialization, SMCs incursion in the tunica media, and vascular remodeling for tissue engineering.

1. Introduction

Synthetic vascular grafts are often limited when the inside diameter of the grafts are smaller than 5 mm, because of the recurrent thrombosis and occlusion.[1] When compared to autografts, the lack of endothelialization of synthetic grafts often results in low patency rate, especially for long-term periods.[2] Thus, the idea of combining different structures and materials to construct multicomponent tissue-engineered vascular scaffolds for improved mechanical properties and biocompatibility has been intensively exploited.[3-6] Zhang[7] and Han[6] developed the dual-delivery of VEGF and PDGF by double-layered electrospun membranes for blood vessel regeneration, which synergistically promoted VECs and VSMCs development on the lumen and exterior of vascular grafts respectively. The specially prepared fibrous scaffold in multilayer could benefit blood vessel reconstruction. Yao[8] improved the PCL/chitosan hybrid small-diameter vascular grafts with sustained heparin release, and the evaluation confirmed the anti-thrombogenic property and endothelialization of heparin functionalization. Fu[9] prepared electrospun gelatin/PCL and collagen/PLCL scaffolds and evaluated the applicability for vascular tissue engineering. It is proved that nanofibrous collagen/PLCL membranes with favorable mechanical and biological properties may be desirable for vascular tissue engineering.

Therefore, an ideal small-diameter vascular graft should have two main advantages. The first is scaffold-based, meaning that it should take advantages of both biological and synthetic materials to determine the outcomes of natural morphology and architectures, suitable mechanical properties, improved biocompatibility, and matched biodegradability.[3] The second is cell-based strategy. Fast endothelialization and SMCs development, as well as high patency rate were expected to be promoted by adding growth factors (e.g. vascular endothelial growth factors, platelet-derived growth factor-bb, and fibroblast growth factor),[7, 10] peptides derived from adhesion proteins, or extracellular matrix (ECM) molecules including collagen, fibronectin, and polysaccharide.[11-13] Electrospinning has emerged as a popular technique to fabricate nanofibrous scaffolds for vascular reconstruction, due to the simulation of the microstructure in native arteries and the availability of integration between grafts and surrounding cells and tissues.[2, 11, 14-16] In addition, it is convenient to adopt natural biomaterials as raw materials during the electrospinning process and the regulatory growth factors or anticoagulants (e.g. heparin, hirudin) are also easy to be incorporated into the grafts.[8, 11, 17, 18]

The antithrombotic performances of heparin release and endothelialization on the luminal surface were most intensively studied.[8, 19-22] Heparin functions in the early periods after implantation, while the long-term patency mainly depends on the rapid endothelialization on the lumen. Promotion of the grafts materials to the quick endothelialization in lumen is of critical importance for the vascular reconstruction. Furthermore, the incorporated growth of ECs and SMCs has been proved to be critical for the successful grafting.[23] It is known that ECs affect abundant physiological processes including thrombosis, platelets and monocytes activation/inhibition, SMCs migration/proliferation and blood pressure.[24, 25] On the other hand, SMCs are regarded

[a] State Key Laboratory for Modification of Chemical Fibers and Polymer Materials, College of Chemistry, Chemical Engineering and Biotechnology, Donghua University, Shanghai 201620, China
[b] Department of Emergency and Critical Care Medicine, Shanghai Tenth People's Hospital, Tongji University, Shanghai 200072, China
[c] State Key Laboratory of Bioreactor Engineering, School of Resources and Environmental Engineering, East China University of Science and Technology, Shanghai 200237, China

Journal of Materials Chemistry B Accepted Manuscript

Please do not adjust margins

essential for functional vascular media engineering, and for ECM deposition and remodeling.[24, 26] Therefore, the challenge is always to encourage cells growth and tissue regeneration *in vivo*, while keeping patency and preventing acute thrombosis and restenosis in the application of tissue-engineered vascular grafts.[3, 19]

Our previous study has found that in electrospun P(LLA-CL)/COL/CS composite scaffolds, well matched mechanical properties and optimal ECs viability were reached especially when the weight ratio of P(LLA-CL) to COL/CS was 3:1.[27] Based on such findings, further evaluation of the P(LLA-CL)/COL/CS scaffolds was conducted both *in vitro* and *in vivo*. Heparin was loaded in the grafts using coaxial electrospinning for the inhibition of early thrombosis. In vivo patency of the grafts was compared by color Doppler flow imaging (CDFI) and digital subtraction angiography (DSA). Immunohistochemical analysis, collagen detection, RT-PCR, and western blot assay were conducted to systematically study the ECs/SMCs growth and vascular-related tissue reconstruction.

2. Experimental

2.1 Fabrication of P(LLA-CL)/COL/CS Composite Scaffolds

P(LLA-CL)/COL/CS composite scaffolds with the ratio of 3:1 and 1:1 (w:w, P(LLA-CL) to COL/CS) were fabricated as previously described.[27] Briefly, P(LLA-CL) with 50% L-lactide (3×10^5 Da, Gunze Limited, Japan) and collagen type I (1×10^5 Da, Sichuan Ming-rang Bio-Tech Co., Ltd, China) were dissolved in 1,1,1,3,3,3-hexafluoro-2-propanol (HFIP, Fluorochem Ltd, UK), while chitosan (1×10^6 Da, 85% deacetylated, Jinan Haidebei Marine Bioengineering Co., Ltd, China) was dissolved in HFIP and trifluoroacetic acid (TFA, Sinopharm Chemical Reagent Co., Ltd, China) (v:v, 9:1) at concentrations of 8% (w/v). The COL/CS ratio in the blending solution was set constant as 4:1. Before electrospinning, P(LLA-CL) and COL/CS solutions were mixed at the ratio of 3:1 (w:w) and 1:1 (w:w) and the grafts acquired were called as 3:1 and 1:1 composite grafts. A syringe pump (789100C, Cole-Pamer, Chicago, IL) and a high voltage power supply (BGG6-358, BMEICO, China) was applied for the electrospinning process. The composite nanofibers were crosslinked for 48 h using glutaraldehyde vapor (GA, 25%, Sinopharm Chemical Reagent Co., Ltd, China) and stored in a vacuum-drying oven. Pure P(LLA-CL) scaffolds were fabricated as the controls.

2.2 Scaffolds Characterization

The morphology of the composite nanofibers was observed using Scanning electron microscopy (SEM) (JEOL JSM-5600, Japan). The chemical structure and composition of the nanofibers were inspected by the Fourier transform infrared attenuated total reflectance spectroscopy (FTIR-ATR) (NEXUS-670, America). The suture retention strength with a 5-0 polyester suture (Shanghai Pudong Jinhuan Medical Products Co., Ltd, China) was tested by a micro material testing machine (MMT-250N, Shimadzu Co., Japan) with reported methods.[28]

2.3 Biodegradability in Vitro

Different scaffolds were cut into rectangles (60 mm×20 mm) for biodegradability test within the scheduled time (150 days). The samples were placed in the phosphate buffered solution (PBS, pH = 7.2 ± 0.1) with sodium azide in a 37 ℃ water bath. SEM was used to observe the morphology change during degradation process. The weight loss percentages were calculated using the following relationships by gravimetrical method:

$$\text{Weight loss (\%)} = \frac{W_0 - W_d}{W_0} \times 100\%$$

Where W_0 is the intial weight and W_d is the dry weight after degradation. The pH value of degradation solution in each month was measured by the digital pH meter (PHS-3C, China). Three specimens were averaged for each sample.[29]

2.4 Cell Viability and Morphology

Human smooth muscle cells (hSMCs, purchased from the Institute of Biochemistry and Cell Biology, Chinese Academy of Sciences, China) were seeded on different electrospun scaffolds in 24 well plates, at a density of 3×10^4 cells/well in 800 μL of Dulbecco's modified Eagle's medium (DMEM, Gibco Life Technologies Co., USA) with 10% fetal bovine serum and 1% antibiotic-antimycotic in an atmosphere of 5% CO_2 and 37 ℃. After culture for 5 days, 4', 6'-diamidino-2-phenylindole hydrochloride (DAPI, Invitrogen, USA) and rhodamine-conjugated phalloidin (Invitrogen, USA) were practiced to stain the nuclei and cytoskeletons of cells, and then the samples were observed using confocal laser-scanning microscopy (CLSM, Carl Zeiss LSM 700, Germany). The 3-(4,5-dimethyl-2-thiazolyl)-2,5-diphenyl-2H-tetrazolium bromide (MTT) assay was performed to test cell viability. After 1, 3, or 5 days of cells seeding, the cells and matrices were incubated with 5 mg/ml MTT for 4h. 500 μL dimethyl sulfoxide (DMSO) solution was then mixed to dissolve the crystals. The UV absorbance values of 492 nm were measured by an Enzyme-labeled Instrument (Multiskan MK3, Thermo, USA). Mouse fibroblasts (L929 cells, purchased from the Institute of Biochemistry and Cell Biology, Chinese Academy of Sciences, China) were also seeded at a density of 1×10^4 cells/well in the same culturing condition. Cell morphology was observed using CLSM after culturing for 5 days. Cell viability was measured by MTT assay after 1, 3, and 5 days.

2.5 Fabrication and Characterization of Heparin Loaded Vascular Grafts

Heparin (1.3×10^4 Da, Runjie Chemical Co., Ltd, China) was dissolved in the distilled water at a concentration of 15%. Heparin-loaded vascular grafts were fabricated using a custom-built electrospinning instrument with a coaxial setup. In the coaxial electrospinning process, heparin was injected at the flow rate of 0.2 mL/h, while the shell solution was injected at 1.0 mL/h. A rotating stainless mandrel collector (4 mm in diameter) was used to collect nanofibers. Heparin-loaded P(LLA-CL)/COL/CS vascular grafts were also crosslinked by means of GA vapor and stored in a vacuum-drying oven. FTIR-ATR measurement was performed on the grafts with heparin, and the suture retention forces were also tested as described in 2.2.

2.6 Implantation

Eight healthy Beagle dogs weighing 15-20 kg were applied as the bilateral femoral artery replacement models in this study. All experimental procedures involving animals in this study were conducted under institutional guidelines for animal care and approved by the Animal Ethics Committee of Shanghai Tenth People's Hospital (Shanghai, China). For each Beagle dog, the P(LLA-

Journal of Materials Chemistry B Accepted Manuscript

This journal is © The Royal Society of Chemistry 20xx

Please do not adjust margins

CL)/COL/CS-heparin vascular graft was implanted into the right femoral artery, and the P(LLA-CL)-heparin vascular graft was implanted into the left one as control, as earlier described.[20] One dog was used for the autologous implantation.

Color doppler flow imaging (CDFI) was performed continually to picture the patency of the implanted grafts after 1, 4, 8 and 12 weeks. Digital subtraction angiography (DSA) was implemented to further compare the patency of different vascular grafts at 20 weeks. For the analyses of explanted grafts, the animals at 12 weeks were killed humanely by overdosed pentobarbital and the grafts were extracted.

2.7 Analyses of Explanted Grafts

2.7.1 Histological investigation. The cross-sectional segments of the implanted grafts were sliced and fixed with 4% paraformaldehyde, and then cut into paraffin-embedded sections. Hematoxylin and eosin (H&E) staining was performed by the conventional procedures. Immunohistochemistry assay with anti-von Willebrand factor (vWF, Abcam, UK) and anti-alpha-smooth muscle actin (α-SMA, Abcam, UK) was also performed on the sections. Then the Biotin-Streptavidin HRP Detection Systems (SP-9000, ZSGB-BIO, China) were incubated with the samples, followed by hematoxylin redyeing and observation by the light microscope.

2.7.2 Collagen detecting. Representative paraffine sections of exposed grafts were dewaxed and then washed with distilled water. The samples were stained in 0.1% picosirius red staining solution for 1 h and washed with distilled water for 5 minutes, followed by counter staining using Harris hematoxylin for dyeing nucleus. The samples were then dehydrated with gradient concentrations of ethanol and sealed using neutral balsam (Mounting Medium). Transparency of the samples was increased by xylene. The observation was performed under the polarized light to identify collagen organization and maturation.[3] The hydroxyproline assay kit (Nanjing Jiancheng Bioengineering Institute, China) was used to evaluate the total collagen amount.

2.7.3 Reverse transcriptase-polymerase chain reaction (RT-PCR). Total RNA was extracted using a total RNA extraction kit (Tiangen Biotech, China), and then RNA (1.0 μg) was reverse-transcribed into cDNA using the M-MLV reverse transcriptase (Promega, USA). Expression levels of vascular related genes including type I collagen (Collagen I, Abcam, UK), type III collagen (Collagen III, Abcam, UK), and endothelial nitric oxide synthase (eNOS, Abcam, UK) were detected by a PCR amplifier (FGEN02TD, Techne, UK). Glyceraldehyde 3-phosphate dehydrogenase (GAPDH) was used as an internal control, and the primers are listed in Table 1. The PCR products were studied by the 2% agarose gel electrophoresis. After checking RT-PCR products, the band intensities were measured and quantified by the Image J software (National Institutes of Health, USA). All measurements were performed in triplicate and the band intensity ratios were calculated through dividing the intensities of Collagen I, Collagen III, or eNOS by those of GAPDH.[30]

Table 1. The primer sequences for amplification.

Gene/Oligo Name	Oligo Sequence
Collagen I forward	5'- CCTGGAAGAGATGGTGCT -3
Collagen I reverse	5'- CCATTCTTGCCAGCAGGAC -3'
Collagen III forward	5'- TGGCATTCCTCCGACTT -3'
Collagen III reverse	5'- CCATCCTCCAGAACTGTGTAT -3'
eNOS forward	5'- AGCCCGGGACTTCATCAATC -3'
eNOS reverse	5'- TGAAGCCGCTGCTCATGAG -3'
GAPDH forward	5'- TGGCGCTGAGTACGTCGTG -3'
GAPDH reverse	5'- ATGGCATGGACTGTGGTCAT -3'

2.7.4 Western blot analysis. Cells and tissues on the explanted grafts were homogenized in the lysis buffer, and total proteins were collected by centrifuging at 10000-140000 rpm for 5 min (Thermo Fresco 17, USA). The total protein of the cell lysate was quantified by the BCA protein assay kit (Thermo, USA). Then the total tissue protein was electrophoresed, transmembraned, and visualized as the conventional procedures of western blot.[31] The expressions of Collagen I, Collagen III, and eNOS in regenerated vascular tissues were detected with GAPDH as protein loading control.

2.8 Statistics Analysis

Statistics analysis was performed using origin 8.0 (Origin lab Inc., USA). All the values were averaged at least in triplicate and expressed as means ± standard deviation (SD). Statistical differences were determined by the analysis of One-Way ANOVA and differences were considered statistically significant at $p < 0.05$.

3. Results and discussion

3.1 Scaffolds Morphology

Fig. 1A displays the flow diagram of electrospinning process for nanofibrous mats. The SEM images and fiber diameter distributions of pure P(LLA-CL), 3:1 and 1:1 P(LLA-CL)/COL/CS scaffolds are respectively shown in Fig. 1B and C. The composite scaffolds had a nano-scaled structure with an average diameter of 408 ±67 nm (3:1) and 328 ± 44 nm (1:1), while pure P(LLA-CL) fibers were of micro scale with an average diameter of 1334 ± 315 nm. As our previous study described,[27] the pure P(LLA-CL) scaffold had larger pore diameter (2.2 ± 0.7 μm) than the 3:1 (1.1 ± 0.5 μm) and 1:1 (0.8 ± 0.4 μm) P(LLA-CL)/COL/CS scaffolds. These outcomes were primarily resulted from the increased conductivity of electrospinning solution with the existence of collagen and chitosan.[32]

Journal of Materials Chemistry B Accepted Manuscript

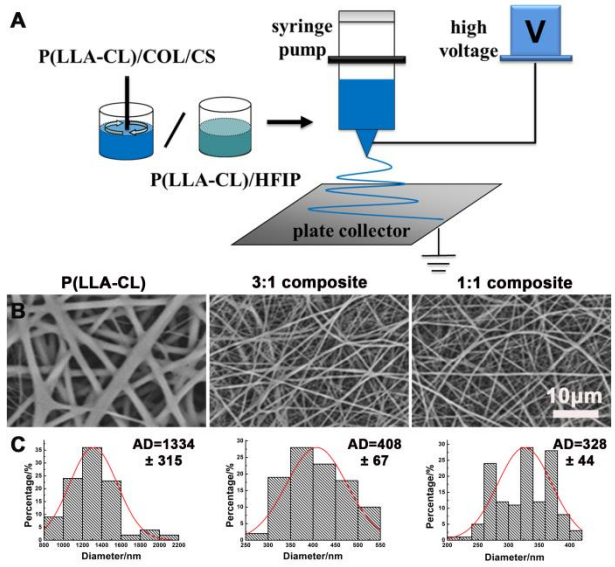

Fig. 1 (A) Diagram of electrospinning process for the fibrous mats. SEM images (B) and fiber diameter distributions (C) of the P(LLA-CL), 3:1, and 1:1 P(LLA-CL)/COL/CS composite scaffolds.

3.2 Scaffolds Characterization

Collagen and polysaccharides are the main components of ECM, which possessed high biocompatibility to promote cells adhesion and proliferation. For the cell culture and further clinic application, the composite scaffolds with collagen and chitosan were crosslinked using GA vapor for optimized crosslinking time (Table S1, supplementary material). To determine whether the chemical structure of collagen and chitosan were altered after crosslinking, FTIR-ATR was utilized to analyze the characteristic absorption peaks of the amide groups and the diffraction peaks. It was found that the collagen and chitosan nanofibers maintained the characteristic groups of the original biomacromolecule (Fig. 2A).The characteristic absorption bands of collagen were observed at 1651 cm^{-1} (amide I), 1538 cm^{-1} (amide II), 1201 cm^{-1} (amide III), respectively while the peak at 1130 cm^{-1} was assigned to chitosan for its saccharine structure. The absorption peak at 3293 cm^{-1} was characteristic of -OH and –N-H vibration.[33]

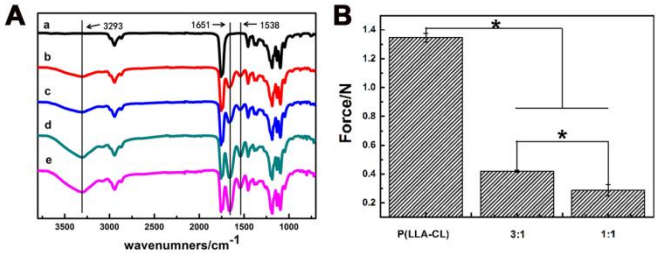

Fig. 2 (A) FTIR spectra of P(LLA-CL) (a), 3:1 (b, c), and 1:1 (d, e) composite scaffolds before (a, b, d) and after crosslinking (c, e). (B) Suture retention forces of different scaffolds.

As previous study showed, the composite scaffold with the ratio of 3:1 matched mechanical properties (tensile stress and elongation, burst pressure and dynamic compliance) with native blood vessels, but the 1:1 scaffold had significant lower ($p<0.05$) tensile stress than the 3:1 composite scaffold.[27] This study further tested the suture retention force in wet state(Fig. 2B). At the same thickness of 0.054 ± 0.001 mm, P(LLA-CL) nanofibers had the largest suture retention force (1.34 ± 0.03 N). Decreasing the proportion of P(LLA-CL) from 75% to 50% resulted in a reduced suture retention force from 0.42 ± 0.01 N to 0.29 ± 0.04 N. The mechanical properties demonstrated the potential application of 3:1 composite scaffolds for human blood vessels.

3.3 Biodegradability in vitro

Fig. 3A shows the SEM micrographs of pure P(LLA-CL), 3:1 and 1:1 composite scaffolds during the degradation process. Pure P(LLA-CL) nanofibers began to swell after 30 days of degradation. After 150 days, no fibrous morphology could be observed. However, fibers in 3:1 and 1:1 scaffolds presented distinct crimping and inter-bonding from the beginning of the degradation. The swelling and bonding of the fibers filled up the internal pores and the fibrous morphology were barely observed from 30 days to 90 days. The swelling extent of the 3:1 scaffold was larger than that of 1:1, as more P(LLA-CL) were blended in the 3:1 scaffold. After degradation for 150 days, most fibers on the 3:1 composite surface lost the original morphology, but some fibers fractured on the 1:1 composite scaffolds with some crystal particles in the surfaces, because collagen and chitosan accounted for half of the amounts and their crystalline region caused the breakage of fibers during the degradation.[29, 34, 35]

The mass loss ratio was shown in Fig. 3B. Pure P(LLA-CL) scaffolds had the lowest mass loss ratio of 24% after 150 days. This was mainly because that the polymer chains in P(LLA-CL) were hydrolyzed to short chains but the degradation products of P(LLA-CL) were insoluble in PBS. In comparison, mass loss ratios of composite scaffolds were up to 28%, which could be attributed to the presence of hydrophilic COL/CS. The presence of hydrophilic material in the nanoparticles allows fast influx of water molecules and build-up of osmotic pressure within the nanoparticle matrix resulting in a reduction of the lag phase. [36] Fig. 3C was the pH value change of each time point. The pH value of pure P(LLA-CL) scaffolds kept decreasing during degradation, mainly because that P(LLA-CL) was the block copolymer of PLLA and PCL and composed of some acidic chain segments.[34] The pH values of 3:1 and 1:1 composite scaffolds fluctuated in a near-neutral range, due to the neutralization of hydrolytic products from COL/CS.

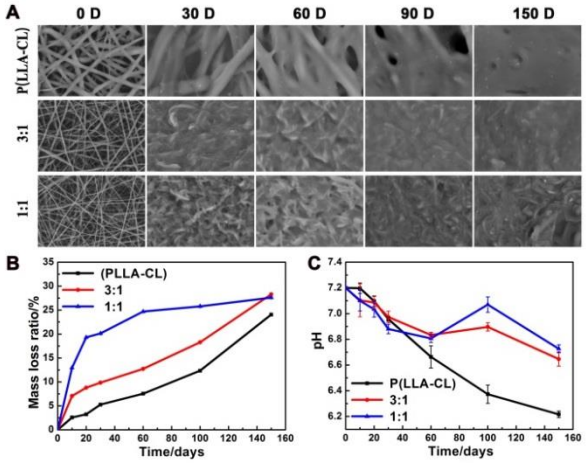

Fig. 3 (A) SEM images of the fibers morphology in the P(LLA-CL), 3:1, and 1:1 composite scaffolds during the degradation of 150 days. (B) The mass loss ratio. (C) The pH value change.

Journal of Materials Chemistry B Accepted Manuscript

This journal is © The Royal Society of Chemistry 20xx

Please do not adjust margins

3.4 Cell Viability

The endothelial cells were found to proliferate and spread better on the 3:1 and 1:1 composite scaffolds than on pure P(LLA-CL) ones, mainly owing to the biologically functional groups of collagen and chitosan.[27] In this study, the biocompatibility of relative cells including SMCs and fibroblasts were detected on the electrospun scaffolds (Fig. 4). Fig. 4A presented the confocal microscopy photographs after culturing for 5 days. hSMCs had a better stretch on the composite nanofibers than on pure P(LLA-CL) scaffolds. The phenomenon became more apparent on the surface of the 3:1 scaffolds, where hSMCs were fully stretched into shuttle shapes. L929 cells had a faster growth on all the electrospun scaffolds than hSMCs, but the cells were increasingly plumped with the addition of collagen and chitosan components. The proliferation rates of hSMCs and L929 cells on different scaffolds in 5 days were given in Fig. 4C and Fig. 4D. The results confirmed that the natural components in the composite scaffolds significantly promoted hSMCs and L929 cells proliferation than those on pure synthetic materials and coverslip controls, regardless of the culture time. The better cell growth may result from the higher specific surface area of nanofibers and the functional reaction cues of collagen and chitosan.[37, 38]

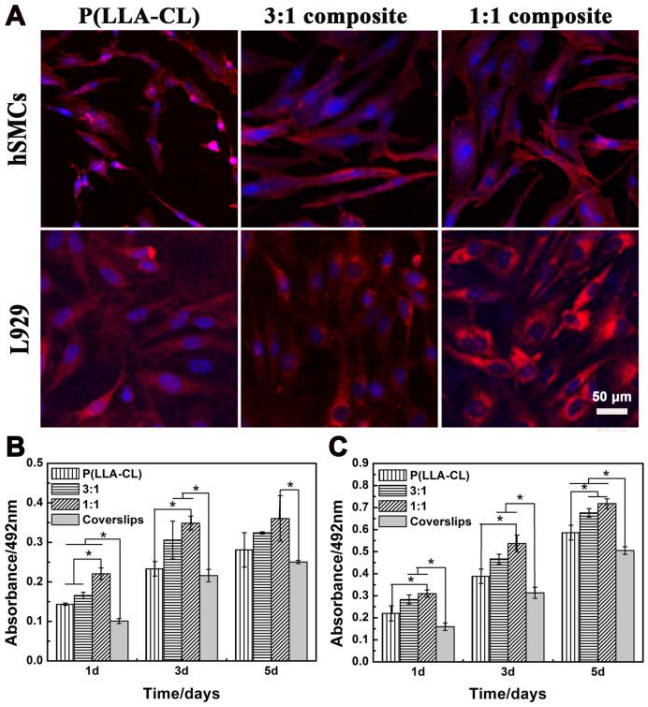

Fig. 4 (A) The confocal microscopy photographs of hSMCs and L929 cells after cultured for 5 days on the P(LLA-CL), 3:1 and 1:1 composite scaffolds. Cell viability of SMCs (B) and L929 cells (C) cultured for 1, 3, and 5 days.

3.5 Heparin Loaded Composite Grafts via Coaxial Electrospinning

As can be seen from the above results, the 3:1 composite scaffolds had slightly lower cell viability but significantly higher mechanical properties than their 1:1 counterparts. Therefore, we selected 3:1 grafts for clinical tests. Heparin was added by coaxial electrospinning (Fig. 5A) to inhibit thrombosis and keep patency in the earlier days after implantation. Fig. 5B and C are the microphotographs, SEM images and fiber distribution of the heparin loaded tubular grafts. The P(LLA-CL)/COL/CS-heparin and P(LLA-CL)-heparin tubular grafts, having an inner diameter of 3 mm and a length of 5 cm, were used for implantation. SEM images and fiber distribution analysis suggested a larger diameter of P(LLA-CL)-heparin fibers, when compared to that of P(LLA-CL)/COL/CS-heparin fibers. In vitro heparin release tests displayed that the coaxial electrospinning method could incorporate heparin in the scaffolds and heparin could be sustained released for more than 20 days (Fig. 5D). FTIR spectra showed the typical absorption peak of heparin at 1640 cm^{-1} caused by –C=O stretching of $–CONH_2$ group. The overlap of $–CONH_2$ in the range of 1640 - 1690 cm^{-1} could be attributed to the characteristic peak of both heparin and COL/CS in P(LLA-CL)/COL/CS-heparin grafts (supplementary material, Fig. S1, A). The suture retention strength of P(LLA-CL) graft was larger than the P(LLA-CL)/COL/CS-heparin one, mainly because of its larger contents of elastic P(LLA-CL) (supplementary material, Fig. S1, B).

3.6 Patency Rate of the Implanted Grafts

Fig. 6A exhibits the surgical implantation of the electrospun vascular graft into the femoral artery of a Beagle dog. Fig. 6B are the typical CDFI tracing images of the blood inflow into the arteries. Clear blood flow was observed smoothly passing through the P(LLA-CL)/COL/CS-heparin tubular grafts in 1, 4, 8 and 12 weeks. The comparison of the patency in the left and right artery in one dog was shown in the DSA image (Fig. 6C). Blood flow was blocked when passing through the P(LLA-CL)-heparin graft, but it was able to get through the P(LLA-CL)/COL/CS-heparin graft in 20 weeks. Based on the results of CDFI and DSA, patency rates at pre-determined time points are illustrated in Fig. 6D. The autologous artery showed a high patency of 100% until it was explanted for detecting after 12 weeks. The P(LLA-CL)/COL/CS-heparin and P(LLA-CL)-heparin grafts expressed the same patency rate in the first 8 weeks after implantation (100% in 1 week, 85.7% in 4 weeks, and 57.1% in 8 weeks), owing to the anticoagulation effect from the released heparin in the early periods.[8] However, P(LLA-CL)-heparin graft showed poor patency rate after implantation for 12 weeks (28.6%) and 20 weeks (14.3%). In comparison, the P(LLA-CL)/COL/CS-heparin graft displayed higher patency (42.9% in 12 weeks, and 28.6% in 20 weeks) than the P(LLA-CL)-heparin one, representing a better consistency *in vivo*.

Journal of Materials Chemistry B Accepted Manuscript

Please do not adjust margins

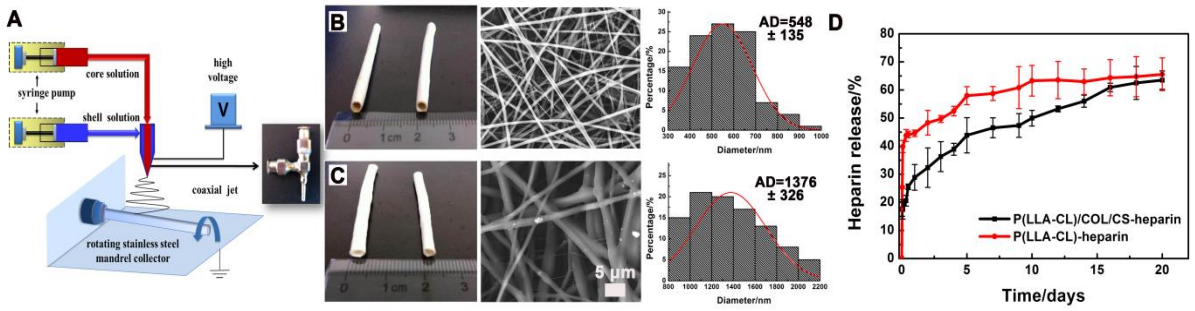

Fig. 5 (A) Schematic diagram of the electrospinning process to fabricate the heparin-loaded grafts. (B, C)The digital photographs, SEM images and fiber distribution of the P(LLA-CL)/COL/CS-heparin (B) and P(LLA-CL)-heparin vascular grafts (C). (D) Heparin release from P(LLA-CL)/COL/CS-heparin and P(LLA-CL)-heparin vascular graft.

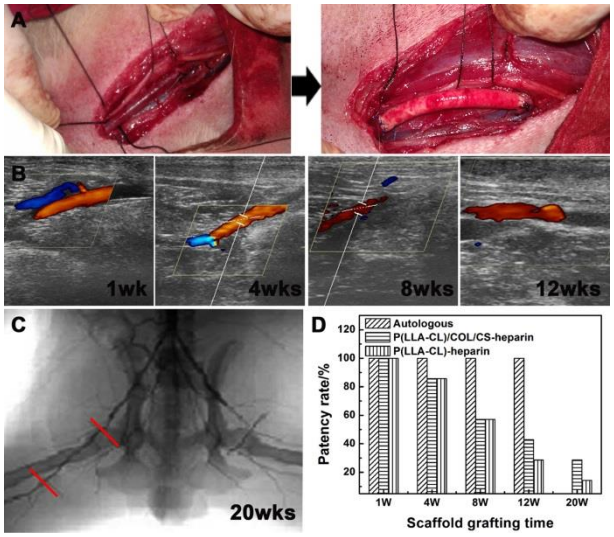

Fig. 6 (A) Surgical implantation of the electrospun vascular graft into the femoral artery of a Beagle dog. (B) The CDFI inspection of the P(LLA-CL)/COL/CS-heparin composite grafts at 1, 4, 8, and 12 weeks. (C) Typical DSA inspection of the P(LLA-CL)/COL/CS-heparin (right) and P(LLA-CL)-heparin graft (left) at 20 weeks. (D) Patency rates of various scaffolds after 1, 4, 8, 12, and 20 weeks of surgical implantation.

3.7 Analyses of Explanted Grafts

3.7.1 Histological analyses

Fig. 7A and B presents the H&E staining images of the implanted grafts at 12 weeks. The lumens of autologous and P(LLA-CL)/COL/CS-heparin graft were fluent, while the P(LLA-CL)-heparin graft was blocked by blood clots. Magnified images in Fig. 7B showed that clear cell monolayers on the surface of both autologous and P(LLA-CL)/COL/CS-heparin graft, and some cells infiltrated into the electrospun grafts. For P(LLA-CL)-heparin graft, no cell growth and infiltration were observed. The immunohistochemical images of vWF and α-SMA further confirmed the results (Fig. 7C and D). For the autologous and P(LLA-CL)/COL/CS-heparin graft, the endothelia cells grew soundly with a cell monolayer covering the entire luminal surface(Fig. 7C). On the contrary, only stacked cells were observed on the P(LLA-CL)-heparin surface. In Fig. 7D, regular and uniform SMCs structures were detected from the autologous and P(LLA-CL)/COL/CS-heparin graft, while no SMCs structure was generated in the P(LLA-CL)-heparin group. These results pointed out that the endothelialization and SMCs development on the P(LLA-CL)/COL/CS-heparin graft were highly matched with those of the autologous grafts, while pure P(LLA-CL)-heparin grafts had poor cell viability.

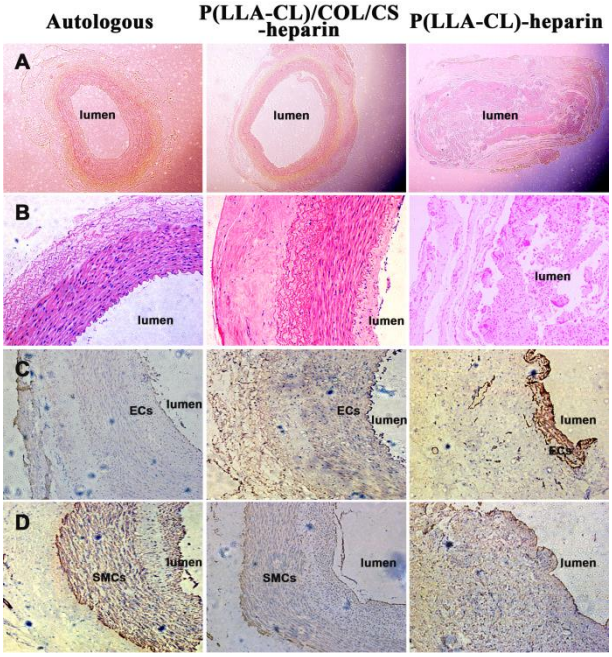

Fig. 7 (A-B) Typical H&E staining images (A: 40×; B: 200×) of the implanted grafts after 12 weeks. Immunohistochemistry images (200×) of vWF (C) and α-SMA (D) of the implanted grafts after 12 weeks.

3.7.2 Collagen detecting

The picrosirius red staining images of the explanted grafts were shown in Fig. 8, and the afresh generated collagen organization in the tissue was evaluated. Fig. 8A and B display the surrounding tissue with oriented structure (birefringent yellow / orange) in the autologous and P(LLA-CL)/COL/CS-heparin graft, demonstrating the presence of mature Type I collagen fibers.[3, 39] In comparison, the blocked P(LLA-CL)-heparin graft showed much less collagen existence and the surrounding structure was random and promiscuous (Fig. 8C). The results of the total collagen contents by the conventional hydroxyproline assay in Fig. 8D further confirmed

Journal of Materials Chemistry B Accepted Manuscript

This journal is © The Royal Society of Chemistry 20xx

Please do not adjust margins

that the autologous and P(LLA-CL)/COL/CS-heparin graft had higher collagen amounts than the P(LLA-CL)-heparin one with a significant difference of $p<0.05$. The P(LLA-CL)/COL/CS-heparin graft even showed a higher collagen amount than the autologous, probably due to the collagen components carried by the fibers themselves.

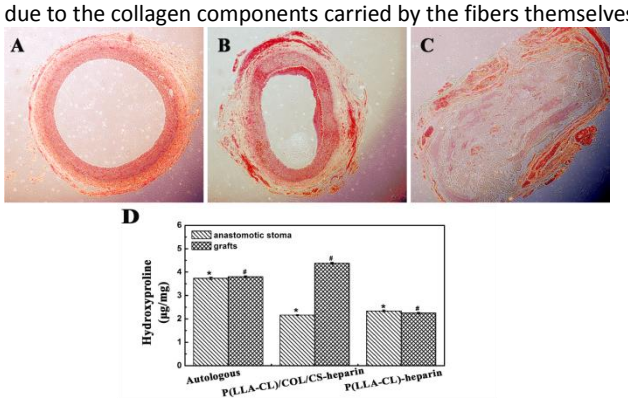

Fig. 8 Picrosirius red staining images of the autologous (A), the P(LLA-CL)/COL/CS-heparin graft (B) and P(LLA-CL)-heparin graft (C) after 12 weeks. (D) Total collagen amounts of the nearby anastomotic stoma and the implanted grafts.

3.7.3 Relative Gene and Protein Expression Induced by P(LLA-CL)/COL/CS Nanofibers

Collagen I, collagen III, and eNOS play important roles in the reconstruction of vascular related structure.[11, 24, 40] Based on the mRNA levels of collagen I, collagen III, and eNOS, the related gene expression of the remolding tissue on the explanted grafts was analyzed at 12 weeks through RT-PCR (Fig. 9A), and the band intensities were quantified and normalized to the expression level of GAPDH (Fig. 9C, D, and E). The collagen I expression level of the autologous (0.96) and the P(LLA-CL)/COL/CS-heparin graft (0.80) was significantly higher than that of P(LLA-CL)-heparin graft (0.59). The nearby anastomotic stoma of the autologous (0.88) had significantly greater collagen I expression than the other two groups (0.74 in P(LLA-CL)/COL/CS-heparin, and 0.68 in P(LLA-CL)-heparin).

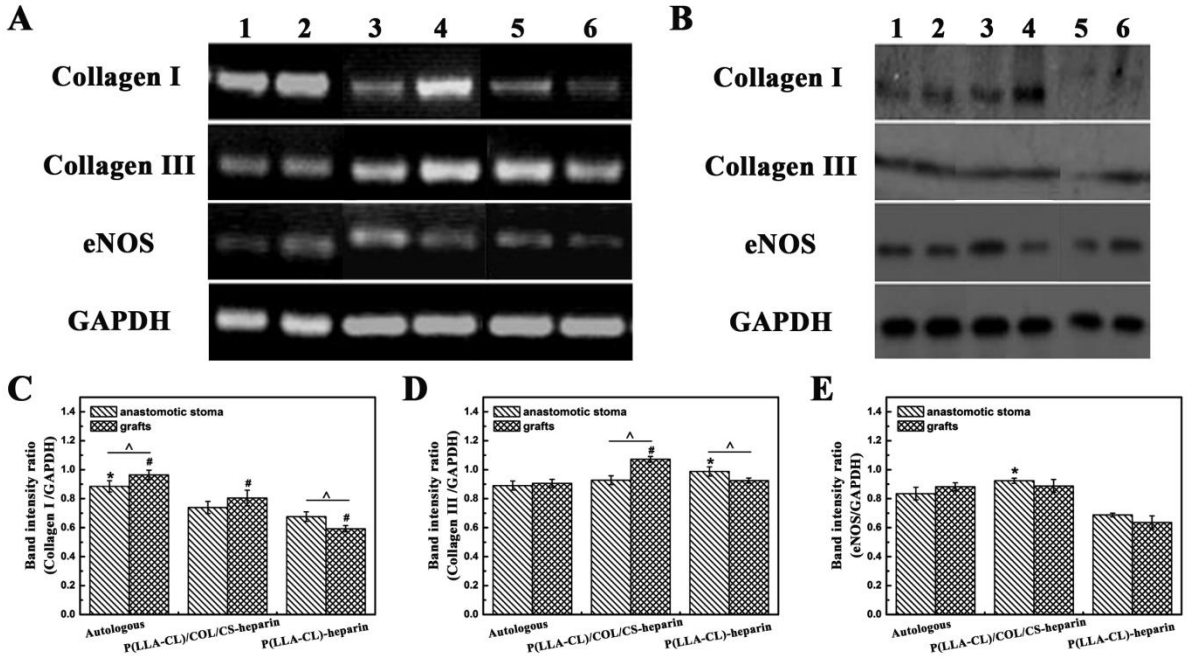

Fig. 9 mRNA expression levels (A) and western blot assay for the protein expressions (B) of collagen I, collagen III, and eNOS in the anastomotic stoma (1, 3, 5) and grafts (2, 4, 6) after 12 weeks (the autologous: 1, 2; the P(LLA-CL)/COL/CS-heparin graft: 3, 4; the P(LLA-CL)-heparin graft: 5, 6; GADPH was used as loading control.). (C-E) Normalized expression levels of collagen I, collagen III, and eNOS mRNA with respect to GADPH expression based on electrophoresis results.

Only the P(LLA-CL)/COL/CS-heparin graft and its anastomotic stoma had comparable collagen I expression level. For collagen III expression, the autologous had no significant difference with its anastomotic stoma (0.91 in the autologous and 0.89 in the anastomotic stoma). However, collagen III was superiorly expressed on the P(LLA-CL)/COL/CS-heparin graft (1.07) than its anastomotic stoma (0.93), while the P(LLA-CL)-heparin graft showed antipodal trend (0.92 in graft, and 0.99 in its anastomotic stoma). The eNOS expression level on each graft was comparable with the autologous, but the anastomotic stoma of the P(LLA-CL)/COL/CS-heparin graft expressed more eNOS than the P(LLA-CL)-heparin one ($P<0.05$). The protein expression of collagen I, collagen III, and eNOS via western blot assay was presented in Fig. 9B. The collagen I and III expression of the autologous and the P(LLA-CL)/COL/CS-heparin graft were both clearly observed, whereas P(LLA-CL)-heparin graft had less collagen expression. The eNOS expression of each group was similar in general, except for the more expression of the anastomotic stoma of the P(LLA-CL)/COL/CS-heparin graft, which confirms the results of RT-PCR. These results revealed that the combination of natural collagen and chitosan in the implanted grafts played a positive role in cells growth, ECM reconstruction and angiogenesis.

Journal of Materials Chemistry B Accepted Manuscript

4. Conclusions

By adjusting the weight ratio of P(LLA-CL) and COL/CS to 3:1 in electrospun vascular grafts, we have found an optimal balance among mechanical properties, biodegradability and biocompatibility. *In vivo* studies further confirmed that the 3:1 composite graft possessed improved long-term patency, better ECs and SMCs development, as well as enhanced vascular-related gene and protein expression in comparison to the pure P(LLA-CL) one. Therefore, the 3:1 P(LLA-CL)/COL/CS composite scaffold provided important insight on the potentials and developments of biodegradable composite vascular grafts. Further cues could be integrated into the structure of such a matrix for the clinical application of in situ vascular tissue engineering.

Acknowledgements

This research was supported by National Natural Science Foundation of China (31470941, 31271035, and 51403033), Science and Technology Commission of Shanghai Municipality (11nm0506200), Ph.D. Programs Foundation of Ministry of Education of China (20130075110005), light of textile project (J201404) and the Fundamental Research Funds for the Central Universities (2232014D3-15).

Notes and references

* Corresponding Author. Tel.: +86 021 67792653.
Email: xmm@dhu.edu.cn (Xiumei Mo),
wangsheng@tongji.edu.cn (Sheng Wang);

[1] Tong Wu and Bojie Jiang contributed equally to this paper.

1. C. K. Hashi, Y. Zhu, G.-Y. Yang, W. L. Young, B. S. Hsiao, K. Wang, B. Chu and S. Li, *Proc. Natl. Acad. Sci.*, 2007, **104**, 11915-11920.
2. J. Yu, A. Wang, Z. Tang, J. Henry, B. Li-Ping Lee, Y. Zhu, F. Yuan, F. Huang and S. Li, *Biomaterials*, 2012, **33**, 8062-8074.
3. M. Stoppato, H. Y. Stevens, E. Carletti, C. Migliaresi, A. Motta and R. E. Guldberg, *Biomaterials*, 2013, **34**, 4573-4581.
4. S. Shinohara, T. Kihara, S. Sakai, M. Matsusaki, M. Akashi, M. Taya and J. Miyake, *J. Biosci. Bioeng.*, 2013, **116**, 231-234.
5. M. J. McClure, D. G. Simpson and G. L. Bowlin, *J Mech Behav Biomed Mater*, 2012, **10**, 48-61.
6. F. Han, X. Jia, D. Dai, X. Yang, J. Zhao, Y. Zhao, Y. Fan and X. Yuan, *Biomaterials*, 2013, 34, 7302-7313.
7. H. Zhang, X. Jia, F. Han, J. Zhao, Y. Zhao, Y. Fan and X. Yuan, *Biomaterials*, 2013, 34, 2202-2212.
8. Y. Yao, J. Wang, Y. Cui, R. Xu, Z. Wang, J. Zhang, K. Wang, Y. Li, Q. Zhao and D. Kong, *Acta Biomater.*, 2014, 10, 2739-2749.
9. W. Fu, Z. Liu, B. Feng, R. Hu, X. He, H. Wang, M. Yin, H. Huang, H. Zhang and W. Wang, *Int. J. Nanomed.*, 2014, 9, 2335-2344.
10. A. Perets, Y. Baruch, F. Weisbuch, G. Shoshany, G. Neufeld and S. Cohen, *J. Biomed. Mater. Res., Part A*, 2003, 65A, 489-497.
11. S. A. Sell, M. J. McClure, K. Garg, P. S. Wolfe and G. L. Bowlin, *Adv Drug Deliv Rev*, 2009, 61, 1007-1019.
12. K. von der Mark, J. Park, S. Bauer and P. Schmuki, *Cell Tissue Res.*, 2010, 339, 131-153.
13. M. Z. Elsabee, H. F. Naguib and R. E. Morsi, *Materials Science and Engineering: C*, 2012, 32, 1711-1726.
14. Z. Wang, Y. Cui, J. Wang, X. Yang, Y. Wu, K. Wang, X. Gao, D. Li, Y. Li, X. L. Zheng, Y. Zhu, D. Kong and Q. Zhao, *Biomaterials*, 2014, 35, 5700-5710.
15. S. de Valence, J. C. Tille, J. P. Giliberto, W. Mrowczynski, R. Gurny, B. H. Walpoth and M. Moller, *Acta Biomater.*, 2012, 8, 3914-3920.
16. T. Pennel, G. Fercana, D. Bezuidenhout, A. Simionescu, T. H. Chuang, P. Zilla and D. Simionescu, *Biomaterials*, 2014, 35, 6311-6322.
17. Y. Su, X. Li, Y. Liu, Q. Su, M. L. W. Qiang and X. Mo, *J. Biomater. Sci. Polym. Ed.*, 2011, 22, 165-177.
18. R. Chen, C. Huang, Q. Ke, C. He, H. Wang and X. Mo, *Colloids Surf. B. Biointerfaces*, 2010, 79, 315-325.
19. W. Zheng, Z. Wang, L. Song, Q. Zhao, J. Zhang, D. Li, S. Wang, J. Han, X. L. Zheng, Z. Yang and D. Kong, *Biomaterials*, 2012, 33, 2880-2891.
20. C. Huang, S. Wang, L. Qiu, Q. Ke, W. Zhai and X. Mo, *ACS Appl Mater Interfaces*, 2013, 5, 2220-2226.
21. M. Avci-Adali, G. Ziemer and H. P. Wendel, *Biotechnol. Adv.*, 2010, 28, 119-129.
22. W. Wu, W. Yao, X. Wang, C. Xie, J. Zhang and X. Jiang, *Biomaterials*, 2015, 39, 260-268.
23. N. L. James, K. Schindhelm, P. Slowiaczek, B. K. Milthorpe, N. P. B. Dudman, G. Johnson and J. G. Steele, *Artif. Organs*, 1990, 14, 355-360.
24. N. Dahan, G. Zarbiv, U. Sarig, T. Karram, A. Hoffman and M. Machluf, *Tissue Eng., Part A*, 2011, 18, 411-422.
25. M. D. K. K. Wu and M. D. P. Thiagarajan, *Annu. Rev. Med.*, 1996, 47, 315-331.
26. L. Jiao, Z. Xu, F. Xu, S. Zhang and K. Wu, *Acta Cardiol.*, 2010, 65, 499-506.
27. A. Yin, K. Zhang, M. J. McClure, C. Huang, J. Wu, J. Fang, X. Mo, G. L. Bowlin, S. S. Al-Deyab and M. El-Newehy, *J. Biomed. Mater. Res. A*, 2013, 101, 1292-1301.
28. H. Bergmeister, C. Schreiber, C. Grasl, I. Walter, R. Plasenzotti, M. Stoiber, D. Bernhard and H. Schima, *Acta Biomater.*, 2013, 9, 6032-6040.
29. K. Zhang, A. Yin, C. Huang, C. Wang, X. Mo, S. S. Al-Deyab and M. El-Newehy, *Polym. Degradation Stab.*, 2011, 96, 2266-2275.
30. J. S. Choi, K. W. Leong and H. S. Yoo, *Biomaterials*, 2008, 29, 587-596.
31. Y. Yang, T. Xia, W. Zhi, L. Wei, J. Weng, C. Zhang and X. Li, *Biomaterials*, 2011, 32, 4243-4254.
32. K. Zhang, H. Wang, C. Huang, Y. Su, X. Mo and Y. Ikada, *J. Biomed. Mater. Res. A*, 2010, 93, 984-993.
33. C. Huang, R. Chen, Q. Ke, Y. Morsi, K. Zhang and X. Mo, *Colloids Surf. B. Biointerfaces*, 2011, 82, 307-315.
34. Y. Dong, S. Liao, M. Ngiam, C. K. Chan and S. Ramakrishna, *Tissue Eng., Part B: Reviews*, 2009, 15, 333-351.
35. Y. Dong, T. Yong, S. Liao, C. K. Chan, M. M. Stevens and S. Ramakrishna, *Tissue Eng., Part A*, 2009, 16, 283-298.
36. G. K. Jain, S. A. Pathan, S. Akhter, N. Ahmad, N. Jain, S. Talegaonkar, R. K. Khar and F. J. Ahmad, *Polym. Degradation Stab.*, 2010, 95, 2360-2366.
37. F. Tian, H. Hosseinkhani, M. Hosseinkhani, A. Khademhosseini, Y. Yokoyama, G. G. Estrada and H. Kobayashi, *J. Biomed. Mater. Res., Part A*, 2008, 84A, 291-299.
38. M. Rafat, F. Li, P. Fagerholm, N. S. Lagali, M. A. Watsky, R. Munger, T. Matsuura and M. Griffith, *Biomaterials*, 2008, **29**, 3960-3972.
39. M. Ahmed, G. Hamilton and A. M. Seifalian, *Biomaterials*, 2014,

Journal of Materials Chemistry B Accepted Manuscript

This journal is © The Royal Society of Chemistry 20xx

Please do not adjust margins

35, 9033-9040.
40. U. Forstermann and T. Munzel, *Circulation*, 2006, **113**, 1708-1714.

Journal of Materials Chemistry B Accepted Manuscript

Please do not adjust margins

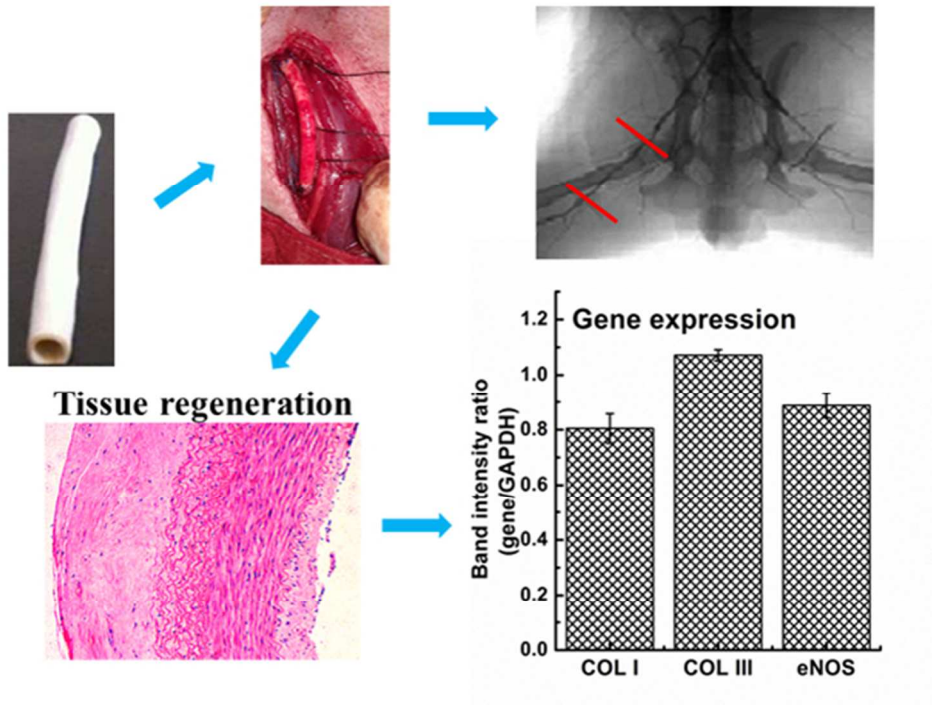

P(LLA-CL)/COL/CS composite vascular grafts could effectively improve patency rate, promote tissue regeneration, and enhance gene expression.
55x39mm (300 x 300 DPI)

Journal of Materials Chemistry B Accepted Manuscript